

THE ANDERSEN IMPACTOR: CALIBRATION, WALL LOSSES AND NUMERICAL SIMULATION

N. P. VAUGHAN

Health and Safety Executive, 403 Edgware Road, London NW2 6LN, U.K.

(Received 7 December 1987; and in final form 24 May 1988)

Abstract—Andersen cascade impactors are widely used to assess airborne particle size distributions. Two forms (MkI and MkII) have been calibrated using solid and liquid aerosols, measured by microscopy, fluorimetry, and aerodynamic particle sizer. A fluorescent tracer was used to examine qualitatively the details of the wall loss deposition patterns when using greased and ungreased plates, and to quantify their magnitude at different particle sizes. The resultant calibrations differ in some respects from the manufacturer's, but are broadly consistent with theory. Suggestions are made for improvements to the design. The results of these investigations were used to produce size-dependent curves for deposition on each plate, and between stages. An entry efficiency curve was assumed. A computer simulation was then performed of the sampling of various log-normal size distributions, so that measured distribution parameters can be corrected for the inevitable imperfections of the impactors. The assumption about entry efficiency is important, but there is little information on this variable, which remains to be determined for the various versions of the Andersen impactor.

NOMENCLATURE

C	Cunningham slip correction
D_j	Jet diameter
d	Diameter of sphere
d_a	Aerodynamic diameter
d_{50}	Diameter at which collection efficiency is 50%
L	Jet length of impactor
N_d	Quantity of material of size d approaching plate
n_d	Quantity of material of size d retained on plate
R	Fractional retention
Re_j	Jet Reynolds Number
S	Jet exit to impaction plate distance
V_j	Air velocity in jet
η	Fluid viscosity
ρ_p	Density of particle
ψ	Stokes Number
$\psi_{50}^{1/2}$	Value of the square root of the Stokes Number at which efficiency is 50%
σ_g	Geometric standard deviation

INTRODUCTION

Determination of airborne particle size distributions is frequently undertaken using cascade impactors. In all such devices, dust laden air is aspirated through a series of impaction stages of successively higher efficiency with respect to aerodynamic diameter. The ideal situation would be where an impaction stage was perfectly efficient in the removal of particles larger than a given diameter, and allowed all particles smaller than this diameter to pass on to the next impaction stage. In practice, for a variety of reasons such a sharp size collection is not possible, and the impaction efficiency of a given stage increases more gradually with increasing particle diameter.

The parameter governing impaction phenomena is the Stokes Number (ψ), given for round jet impactors by:

$$\psi = \frac{C \rho_p d^2 V_j}{18 D_j \eta} \quad (1)$$

From this expression it can be seen that it is the aerodynamic diameter of the particle ($d_a = d_p \rho_p^{1/2}$) which determines whether or not it will be removed by impaction in a given jet, and that aerodynamic diameter is proportional to $\psi^{1/2}$. However, when comparing the efficiencies of impaction jets of different geometry, or the same jet at different flow rates, it is usual to study efficiency with respect to $\psi^{1/2}$ instead of d_a .

Theoretical and experimental studies of impactors by May (1945, 1975), Ranz and Wong (1952), Marple and Willeke (1976) and others have led to the position where impactors can be fairly accurately designed to meet specific size selection requirements. There are, however, a number of uncontrolled and unpredictable factors which may modify impactor performance (such as interaction between adjacent jets, particle bounce, re-entrainment, wall losses and particle deagglomeration; see Rao and Whitby, 1978a, b) and a calibration based solely on theory is inadequate for accurate prediction of overall sampler performance.

The popularity of cascade impactors, probably due to a combination of relative ease of mass distribution measurement (weighing instead of conversion from particle counting), direct *in situ* measurement of aerodynamic diameter (vital in mixed-dust atmospheres) and collection of separate sized fractions of dust for subsequent component analysis, ensures that they will continue to be used extensively.

DEVELOPMENT OF THE ANDERSEN IMPACTOR

One of the most commonly used cascade impactors is that based on the original design of Andersen. This consists of a series of stages having nominally increasing efficiency. Each stage is comprised of a number of identical circular accelerating jets (usually 400) arranged in a circular pattern, which direct incoming particles towards an 82 mm diameter collection plate. Having impinged on the plate, air moves radially outwards to the plate edge, where it must turn through 180° before passing on to the next stage. (Figure 12 shows a section through part of the impactor.) There are however several versions of this instrument in existence, and a brief summary of the development and evolution of the sampler is given below.

(1) Andersen (1958) introduced a six stage cascade impactor, designed to collect airborne bacteria by impacting them onto the surface of agar in petri-dishes, which he calibrated by counting and sizing of collected wax spheres by optical microscopy, quoting simply the 95% size range of particles in each dish.

(2) Andersen (1966) released the same basic design of sampler for use in collecting 'non-viable' particles on stainless steel or glass impaction plates. The chart and table from Andersen (1958) were reproduced in the paper describing this impactor. This paper also stated that: 'the accuracy of these values should suffice for all practical purposes'. It would appear that Andersen had not fully realized the extent to which his sampler would be used, or the degree of accuracy which would be expected in measurement of airborne particle size distributions.

(3) In about 1970 the sampler was redesigned to subdivide incoming dust into 8 fractions (stages 0-7) and an integral back-up filter included. This version became known as MkI (Fig. 1).

(4) In 1977 the MkII version of the sampler (Fig. 2) was released, following work by McFarland (1977) and McFarland *et al.* (1977), who suggested redesign of the top two stages, and the use of a preimpactor.

Numerous independent investigators have tested the various forms of the impactors described above (May, 1964; Flesch *et al.*, 1967; Rao and Whitby, 1978b; Esmen and Lee, 1980; Riediger, 1974; Boulaud *et al.*, 1981; Tanaka *et al.*, 1983 and, most recently, Mitchell *et al.*, 1988). The results of many of these investigations highlight the importance of the collection substrate in determining impactor performance, and all arrive at different sets of calibration curves from those given in the operation manual, which quotes the work of Ranz and Wong (1952).

When enquiries were made direct to the manufacturers, they stated that their calibration was based on 'a combination of experimental and theoretical calculations' (Smith, 1984), and

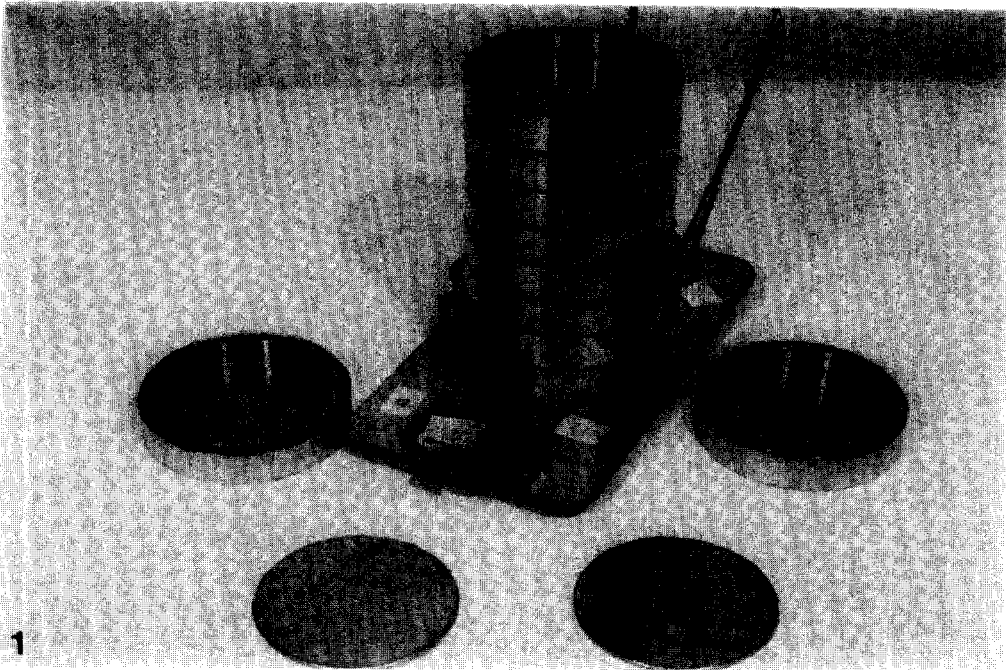


Fig. 1. Andersen MkI eight stage impactor, partly disassembled, showing form of stages and plates 0 and 1.

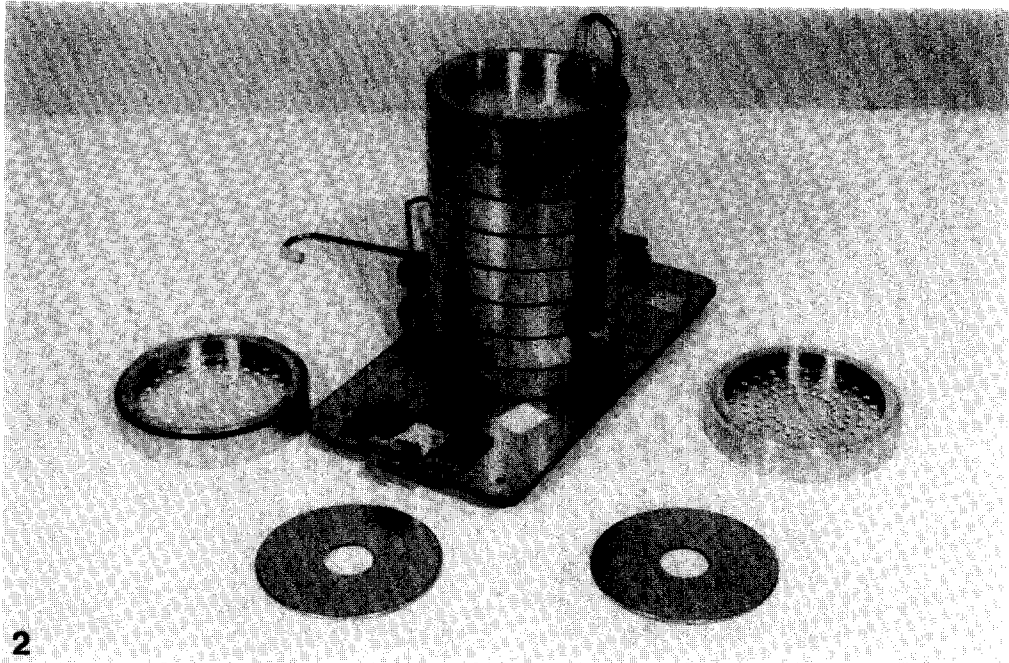


Fig. 2. Andersen MkII impactor, partly disassembled, showing modifications to stages and plates 0 and 1.

cite Andersen (1966) as the source of the calibration of the MkI 8 stage impactor. This 1966 report deals however with the six stage non-viable impactor, the performance of which was assumed to be the same as the original viable impactor. Thus the frequently used calibration for this instrument appears to bear only tenuous relationship to experimental measurements and is most probably based heavily on the curves of Ranz and Wong (1952).

This approach is open to numerous sources of error. The work of Ranz and Wong was based on single jet impactors operating at jet Reynolds numbers (Re_j) in the range 700–23000. The summary of Andersen MkI and MkII impactor parameters in Table 1 shows that this would only apply to stage 7 and the preimpactor. A detailed theoretical model of impactors, developed by Marple and Liu (1974), determined that Re_j was an important factor in determining both the steepness and the position on the $\psi^{1/2}$ axis of the characteristic curve for a given impaction jet. Other factors which Marple and Liu found to have a significant effect on impactor performance are described in Table 2.

The multi-orifice nature of the impactor stages will considerably affect the flow of air away from the impaction points and may alter the impaction efficiency characteristic. The presence of a preceding stage in a cascade impactor constrains the flow of air approaching the jets of subsequent stages, and may again alter the impaction characteristics, although it will probably have more effect on wall losses than size separation.

For these reasons, it is to be expected that the actual performance of the Andersen impactor will differ from that predicted by theory with respect to both the position of the efficiency curve on the axis of $\psi^{1/2}$ (and hence aerodynamic diameter), and the slope of the curve. These effects have been noted by Boulaud *et al.* (1981) who found $\psi_{50}^{1/2}$ to range from 0.25 to 0.37 for the various stages of MkII impactor (excluding the preimpactor), while Ranz and Wong's theory predicts a value of 0.32.

Although only two forms of the Andersen impactor are now commercially available (the 'viable' impactor and the MkII 'non-viable' versions) any of the other versions may still be in use as the device is quite robust. Only the MkI and MkII non-viable samplers were studied in the investigation described here, however.

CALIBRATION METHODS

Calibration of the Andersen impactors (MkI and MkII, 8 stage, using untreated stainless steel plates) was carried out in a 1 m³ static dust box, using a number of different approaches.

Table 1. Summary of impactor jet characteristics

Stage	D_j (cm)	V_j (cm s ⁻¹)	Re_j	S/D_j	L/D_j
Preimp.	1.35	331.6	2976.1	1.26	3.19
MkII 0	0.255	96.3	163.7	0.40	1.78
MkII 1	0.189	175.8	221.2	0.54	2.40
MkI 0	0.159	59.6	63.1	1.37	0.86
MkI 1	0.118	107.7	84.1	1.84	1.08
2	0.091	179.8	109.6	2.37	1.46
3	0.071	297.2	140.9	3.05	1.90
4	0.053	528.9	187.9	4.07	2.46
5	0.034	1277.0	292.0	6.32	3.85
6	0.025	2328.8	394.3	8.54	5.20
7	0.025	4618.1	782.0	8.54	5.20

Table 2. Summary of properties controlling impaction characteristics

Property	Sensitive range	Effect of increase in property
Re_j	< 500	$\psi_{50}^{1/2}$ decreases, curve steepens
L/D_j	< 1.0	$\psi_{50}^{1/2}$ decreases
S/D_j	< 1.0	$\psi_{50}^{1/2}$ increases

These have been described fully in Vaughan (1986a, b), but are summarized below and in Fig. 3.

(1) Monodisperse droplets (σ_g typically < 1.05) of dioctyl phthalate (DOP), fluorescently tagged with Uvitex OB (Ciba-Geigy) in the size range $1.5\text{--}17\ \mu\text{m}$ were produced by a modified Berglund-Liu generator (Berglund and Liu, 1973; Vaughan, 1986a). Size distributions of the test aerosols were individually measured using a microthread technique/optical microscopy (May and Druett, 1968). The quantity of aerosol on each plate of the impactors was assessed by fluorescence spectrophotometry. Results from runs where the measured σ_g exceeded 1.1 were discarded. Measured σ_g s were typically less than 1.06.

(2) Atomized monodisperse polystyrene latex particles (each batch sized by TEM using a semi-automatic image analyser) in the size range $0.3\text{--}13\ \mu\text{m}$ were individually sampled. Test aerosols exhibited σ_g s of less than 1.05. Plate deposits were assessed by one of two methods, according to size. For particles larger than $1\ \mu\text{m}$, deposits were quantitatively transferred to membrane filters, which were then cleared (LeGuen and Galvin, 1981), and the particles counted by optical microscopy. For particles smaller than $1\ \mu\text{m}$, plate deposits were transferred to TEM grids using a quantitative centrifuge technique, and particles counted by TEM.

(3) Polydisperse atomized PVA (hairspray) was collected and measured directly on the impaction plate by means of an optical microscope/image analysis (Magiscan) system. The numbers and sizes of particles in the range $2\text{--}10\ \mu\text{m}$ on each plate were determined.

(4) Polydisperse DOP aerosol was generated by an air blast atomizer, and impaction efficiency assessed by means of an APS 3300 (TSI Inc.) in a similar manner to that subsequently described by Mitchell *et al.* (1988) for monodisperse aerosols. By measuring the size distributions of the test aerosol passing beyond a given impactor stage, with and without the impaction plate in place, retention efficiencies could be deduced. Particle retention for the size range $0.5\text{--}15\ \mu\text{m}$ in 50 intervals could be measured simultaneously, for each stage or combination of stages.

Retention efficiency (R) for each of the methods was assessed by:

$$R = \frac{n_d}{N_d}, \quad (2)$$

where n_d = quantity of aerosol of size d depositing on plate and N_d = quantity of aerosol of size d approaching plate.

Owing to the difficulty in recovery and quantification of particles from the back-up filters of the impactors, it was necessary to assume that plate 7 was 100% efficient at retaining all particle sizes and, as a result, no calibration data is available for this plate. As only plate deposits were analysed, no account was taken of material lost to the impactor walls in these methods. This problem is addressed separately, below.

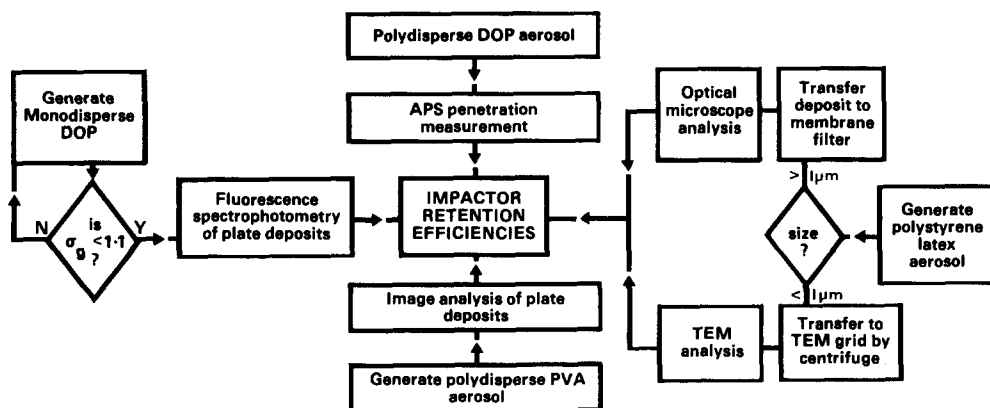


Fig. 3. Diagram showing calibration methods used.

Results from all the methods described above were combined to give a total of over 1000 data points of retention against aerodynamic diameter, or by applying equation (1), against $\psi^{1/2}$.

Figure 4 shows one stage retention curve, measured by the different methods, plotted against the Cunningham-corrected aerodynamic diameter. This curve is typical, in both the relative spread of data points and the degree of agreement between the different methods, of all the impactor stages investigated. (No differences were noted for stages 2 and beyond between the MkI and MkII versions of the impactor, so results for these were combined.) The results show the familiar S-shaped curve, but also, for particles larger than about $5 \mu\text{m}$, occasional values of R of less than 1.0 for both latex and monodisperse DOP aerosols. These values may be due to particle bounce or break-up. The effect is however very variable for particles of the same nominal size, and is therefore difficult if not impossible to quantify. For particle sizes where bounce and break-up did not occur, there was good agreement between the various methods of assessment, and the S-shaped size separation characteristic was obtained.

Plots of retention data such as Fig. 4 were used to define simplified penetration curves for each stage (fitted by eye through the points) from $R=0$ to 1.0. No attempt was made to incorporate the effects of particle bounce. These simplified curves for all measured stages of the MkI and MkII impactors are shown in Figs 5 and 6 respectively, together with the quoted calibration curves taken from the operation manuals. Table 3 summarizes the manufacturer's and measured d_{50} values for each stage, together with values calculated from the theory and experimental findings of Ranz and Wong. Marked differences between quoted and measured calibrations are apparent, especially for stages 0 and 1 of the MkI and stage 2 of both MkI and MkII impactors. In all cases there is a difference between the shapes of the size selection curves. For many curves the measured characteristic is steeper, and the cut-off sharper than that quoted by the manufacturer (i.e. the impactor performs better than claimed), although experimental and quoted d_{50} values are often similar for the lower stages. The long tail to small particle sizes for plate 6 is almost certainly a consequence of assuming complete efficiency for plate 7. (Recalculation of the penetration data of plate 5, assuming 100% efficiency for plate 6, distorts the plate 5 retention curve similarly.) The true curve for plate 6 is probably similar in shape to that of plate 5.

Calculated $\psi_{50}^{1/2}$ values are given again in Table 3. These results indicate a wide variation in the value of $\psi_{50}^{1/2}$, as was found by Boulaud *et al.* (1981).

Comparing the curves with those of Boulaud (1981), and Mitchell *et al.* (1988), there are areas of both agreement and disagreement between all three calibrations. In keeping with tradition, no two calibrations are in complete agreement, although results presented here are

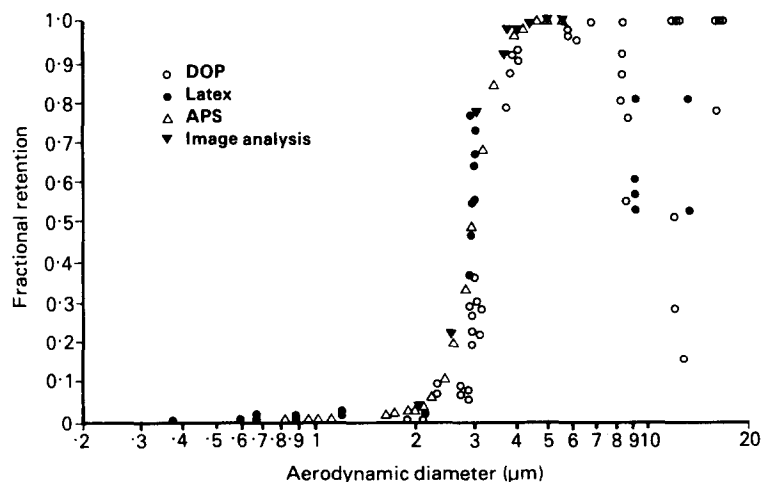


Fig. 4. Combined data for stage 3 of the Andersen impactor.

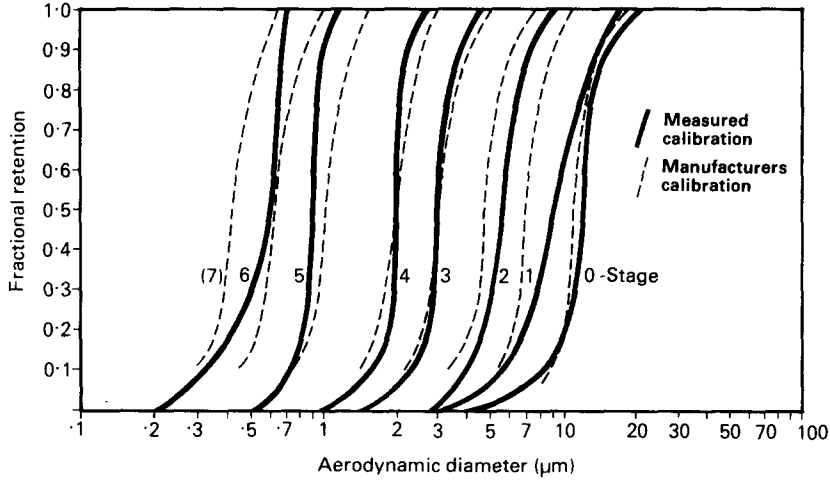


Fig. 5. Mkl Andersen impactor quoted and measured calibration.

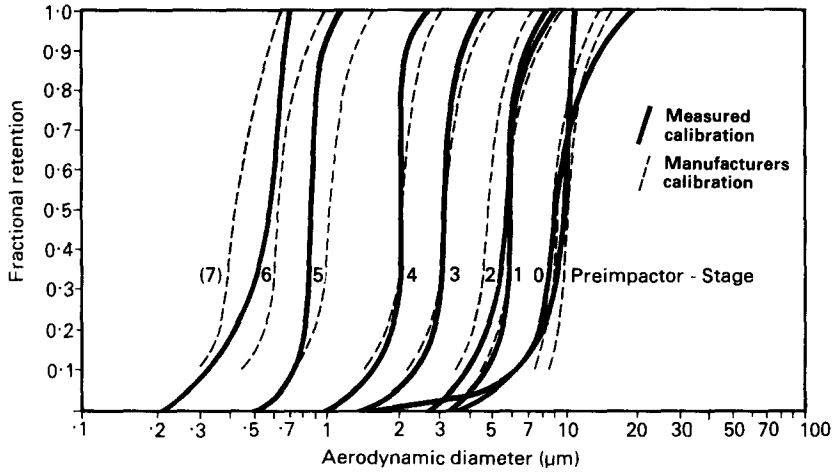


Fig. 6. MkII Andersen impactor quoted and measured calibration.

somewhat closer to those of Mitchell than to those of Boulaud. In practice, and in view of the other factors detailed below, for all but the most detailed applications, such differences are probably unimportant.

By drawing on the findings of other workers in this field (notably Marple and Liu, 1974) which were summarized in Table 2, it should be possible to determine whether the differences between the quoted and observed calibrations are consistent with current impaction theory.

Starting at the top of the MkII impactor (neglecting the preimpactor, owing to its widely different geometry) stages 0 and 1 have relatively low values of Re_j (164 and 221 respectively) which would tend to shift the retention curve to higher values of $\psi^{1/2}$. Their values of the ratio S/D_j are, however, well below 1.0 and this would tend to counteract the effects of low Re_j . On passing to stage 2 however, Re_j falls further to 109.6, but S/D_j exceeds the value of 1.0, above which it becomes unimportant. The retention curve for stage 2 would therefore be expected to lie at a relatively high value of $\psi^{1/2}$ and have a relatively low slope. This is in fact what is observed in the measured calibration.

The effect of Re_j is by far the most important factor in determining the relative position and slope of the retention curves. For the upper stages the effects of the other parameters S/D_j and L/D_j could explain the observed differences from positions predicted by Re_j alone.

It may be concluded therefore that the measured calibration is broadly in agreement with impaction theory.

WALL LOSSES

Since the earliest work on cascade impactors (May, 1945) the phenomenon of wall loss has been recognized as an important source of error in size distribution measurement, the general effect being a bias to small particle sizes. All forms of the Andersen impactor have been shown to exhibit considerable wall losses, especially in the top few stages (May, 1964; Rao and Whitby, 1978b; McFarland, 1977). A series of experiments was conducted in order to:

- (a) Render these wall losses visible so as to determine where, and by what mechanisms, they occur.
- (b) To quantify the wall losses for the MkI and MkII impactors with a view to correcting measured size distributions for their bias.
- (c) To determine the effect of different operating procedures on the magnitude of any wall losses.

The method of visualization chosen was to sample a dust cloud comprised of a commercial phosphor powder (Thorn), and to examine the deposits with u.v. light. The phosphor used exhibited a bright white/yellow fluorescence, and even extremely light deposits, invisible in daylight, were clearly visible under u.v. illumination.

Details of the wall loss visualization and quantification methods used are again given in Vaughan (1986a, b). Investigations were carried out on the MkI, and MkII with and without preimpactor, for heavy and light dust loadings with untreated stainless steel plates, and for light loadings with greased plates.

Wall loss visualization

Several consistent patterns of wall loss were evident on visual examination of the exposed internal surfaces of the impactors. From these, the detailed internal flow pattern of the various forms of the impactor could be deduced. In general, losses occurred mainly in regions of locally converging air flow, or where air was forced to make sharp changes in direction. A few examples are described below.

When using either the inlet cone or the preimpactor on either the MkI or MkII, incoming air is directed towards the top of jet stage 0. Both MkI and MkII show heavy wall loss concentrated in the regions directly beneath the inlets, resulting from the inlet nozzle/stage system acting as an additional impaction stage. The cone tended to concentrate losses in the stage centres (Fig. 7), while the preimpactor produced three concentrations at half the stage radius (Fig. 8). Deposits in the vicinity of the impaction jet entries were concentrated radially outwards from the centres of the preceding inlet regions, and resulted from high inertia particles being unable to turn sharply into the jets from the general diverging air flow, and overshooting the jets (Fig. 9). Tapering of jet inlets in the MkII appeared to have negligible effect.

Under stage 0 of the MkI the only appreciable losses occurred at the extreme edge, where air, having impinged on the first impaction plate, flowed around the edge of the plate and onto the next jet stage. In this region, heavy, circumferentially periodic concentrations of wall loss were seen, resulting from high inertia particles being unable to follow the sharp turn in air flow. The periodicity resulted from the fact that air flowing off the edge of the plate tended to do so between the impaction jets in the outermost ring.

With the MkII, the redesign of the stage permits the passage of air both around the periphery, and through the centre of the plate. As a result, less wall loss is expected at the stage edge, and losses in this region were considerably reduced, although still present. However, passage of air through the plate centre caused a new pattern of deposition in the converging air flow of the central dead space (Fig. 10). Losses were heaviest in this region

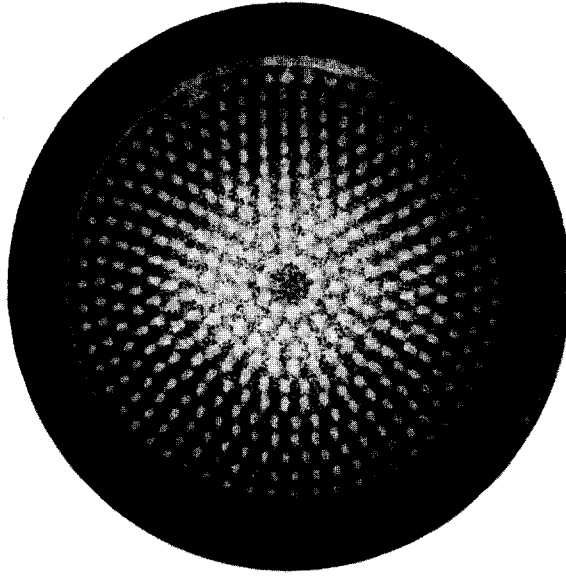


Fig. 7. Wall losses on MkI stage 0, top.

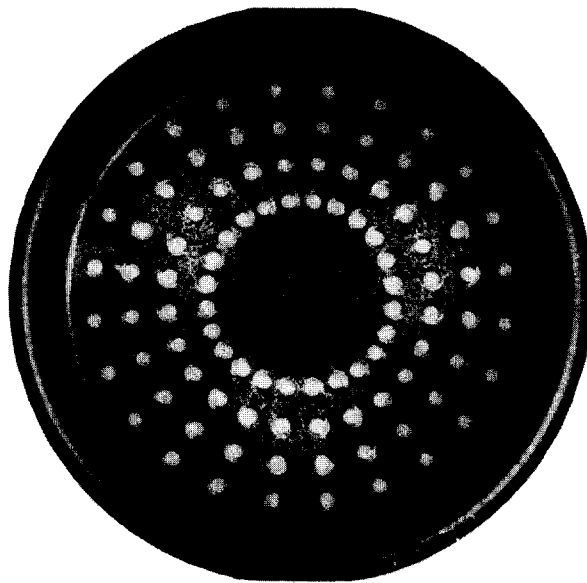


Fig. 8. Wall losses on MkII stage 0, top, using preimpactor

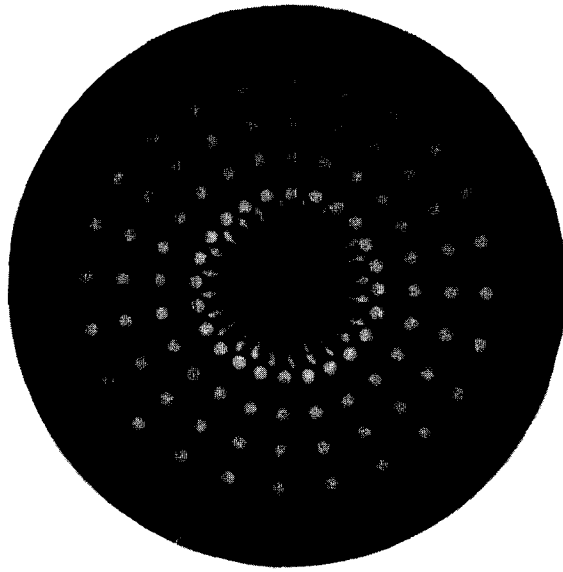


Fig. 10. Wall losses on underside of MkII stage 0.

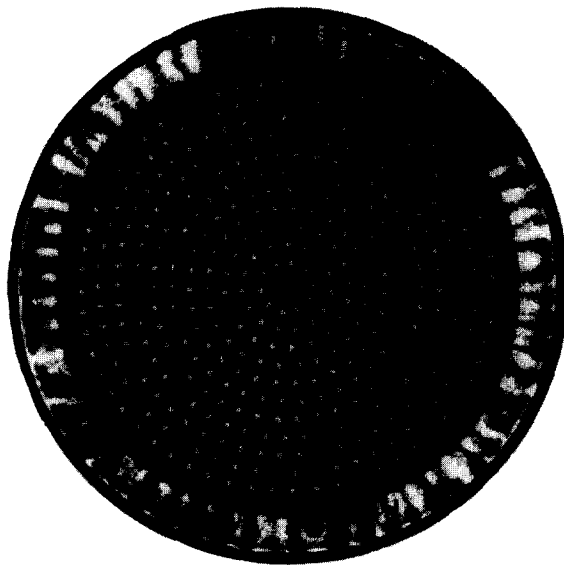


Fig. 11. Wall losses on MkI stage 1, top.

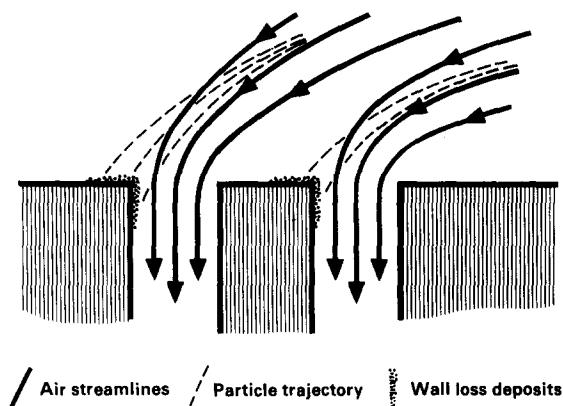


Fig. 9. Diagram depicting wall loss due to overshoot of particles near jet entry.

when using the inlet cone, and were reduced with the preimpactor, where a slight 3-fold symmetry could be made out. Losses at the stage edge were however increased when using the preimpactor, due to the non-central inlets altering the division of flow between the plate centre and edge.

In the MkI, the dominant feature of wall loss on the top of stage 1 was the continuation of the periodic streaks seen on the underside of stage 0 (Fig. 11). Again, overshoot of particles at jet entries revealed the direction of local air flow suggesting an air flow pattern such as that shown in Fig. 12.

In the MkII, as flow was possible through the centre of the overlying plate, heavier losses were noted in the stage centre. These were generally lower when the preimpactor was used.

The pattern of wall loss for stages 3 and beyond of both MkI and MkII impactors were identical, generally being lower for the MkII, and lower still for the MkII with preimpactor, and decreasing in quantity from one stage to the next.

For the lowest stages, a new pattern of losses was evident, which increased in quantity from one stage to the next. This consisted of well-defined light deposits of particles midway between jets on the underside of jet stages and on the underlying impaction plates (Fig. 13), marking out regular cells. These deposits were therefore located in regions of locally converging air flow. The particles in these deposits were far larger than ought to be present at this level in the impactor, and almost certainly represented particles which had bounced or been re-entrained from higher stages. Such deposits on the lower plates will seriously bias any measured mass size distribution to small particle sizes.

Grease

The use of grease (Apiezon H) on the impaction substrate was investigated as a means of wall loss reduction. Such adhesive layers, however, can have no effect on losses until they are first encountered by the dust-laden air. In all three cases (MkI, MkII and MkII with preimpactor) losses and deposits on inlet cones, preimpactor and upper surface of jet stage 0 were the same as before. Undersides of jet stages 0 exhibited the same patterns of losses, but were slightly reduced in quantity. The greatest differences were noticed for the impaction plate deposits themselves. Individual impact points were much better defined than previously, and trailing of deposits was all but absent. Below the level of the first greased impaction plate, wall losses were greatly reduced, although still detectable with careful microscopic examination, and plate deposits continued to be well defined.

This exercise in visualization serves to show the virtual inevitability of wall losses, and provides a number of important lessons for the design and use of particle sampling systems. The elimination of wall losses in the various forms of the Andersen impactor would necessitate a total redesign of the sampler, and is beyond the scope of this work. A number of approaches could, however, prove fruitful for future workers in this field.

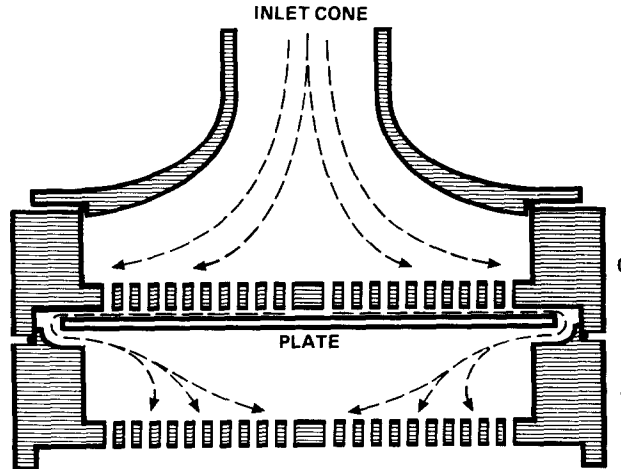


Fig. 12. Schematic section of Andersen MkI impactor, stages 0 and 1, showing air flow pattern inferred from wall loss deposits.

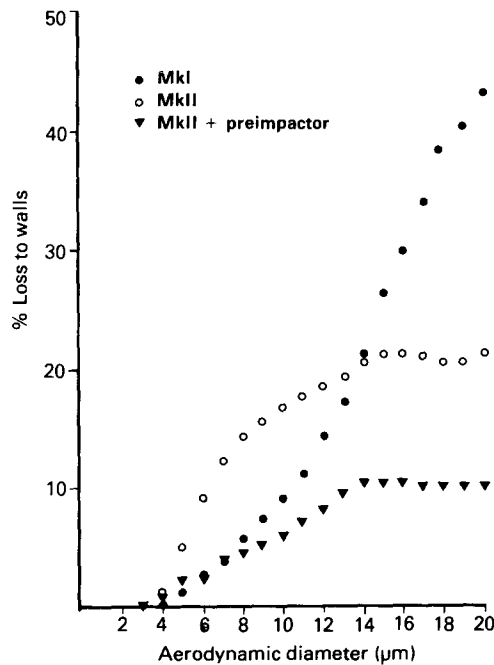


Fig. 14. Proportion of phosphor powder particles of different sizes lost to walls in MkI, MkII and MkII with preimpactor.

(1) Increase the separation between the top of stage 0 and the inlet (whether single or triple). This would reduce the effects of impaction on the jet stage surface, and by decreasing the intensity of divergent air flow, considerably reduce the overshoot of particles in the vicinity of jet intakes. A long tapering inlet was suggested by McFarland (1977) but not taken up by the manufacturers.

(2) Sharp changes of direction in air flow around plate edges should be eliminated by increasing the space available in this region.

(3) Increasing the space above jet stages 1–7 could help reduce the overshoot of particles in the vicinity of jet intakes. Tapering all jet inlets may also prove beneficial.

(4) For the top two stages of the MkII, a redesigned impaction plate with a series of radial slots mid way between the radial rows of impaction jets could remove the central wall losses,

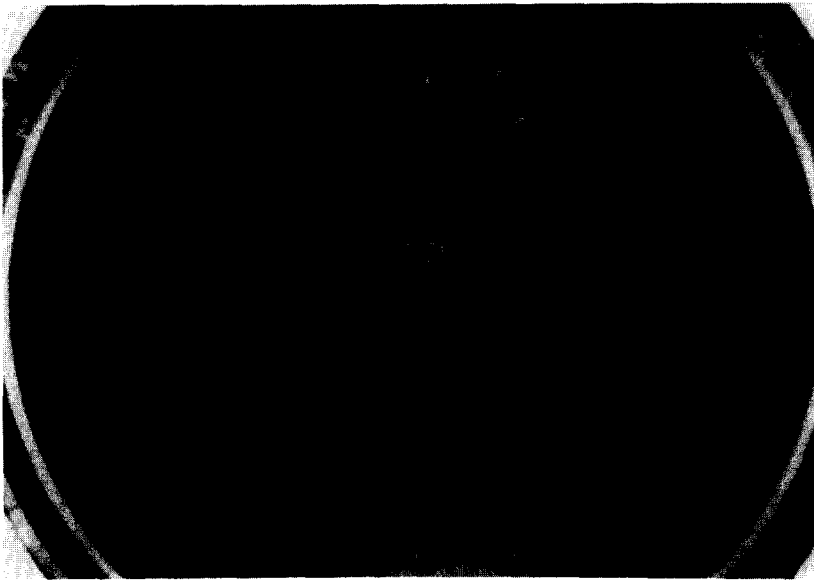


Fig. 13. Diffuse deposits marking out cells on plate 7.

while keeping flow around plate edges low, and still further reduce any effects of radial pressure fall. Exact relative registration of plates and stages would, however, be necessary.

Such changes would undoubtedly result in a heavier, bulkier sampler, which for some applications would be undesirable. The full consequences of any modifications would however require verification both for their effect on overall wall losses and for any effect on efficiency calibration. A case in point is the redesign of the MkI to give the MkII: diversion of air through the plate centre reduced losses near the stage periphery, as expected. Unfortunately, it also introduced a new, unforeseen, mechanism for wall loss in the central dead space.

Quantification of wall losses

Quantitative removal and analysis of the wall losses and plate deposits of phosphor powder was performed by atomic absorption spectroscopy for cadmium. The results of the analyses enable the relative quantities of wall loss and deposit in different locations in the various types of impactor to be determined. For the MkI impactor, regardless of operating conditions, approximately half the incoming dust was lost to the impactor walls, and consequently lost to the analysis of particle size distribution. Without use of the pre-impactor, the wall losses in the MkII could, by keeping plate loadings low and using greased plates, be reduced to approximately a quarter of the material involved. Using the preimpactor, assuming that all the material it collects can be recovered and quantified, again approximately halved the wall losses with the MkII. (It should be stressed that these figures only strictly apply to dusts having the same overall size distribution as the phosphor used in this investigation, i.e. $d_{50} = 40 \mu\text{m}$, $\sigma_g = 1.5$.)

In itself this quantity of wall loss might not be serious, leading only to the need to sample proportionately longer to collect the required quantity of material. The problem with wall losses lies in the fact that, owing to the mechanisms by which they arise, losses generally occur preferentially for larger particles, and measured size distributions will therefore be biased to fine particle sizes. This dependence of wall loss on particle size for the phosphor powder was determined for the Andersen impactors by summing the individual size distributions involved (measured in different wall loss locations by reflected fluorescence microscopy and scaled according to the results of the relevant quantitative analysis). These size-dependent wall losses are shown in Fig. 14. The efficiency of particle removal by wall loss in the various locations was also calculated from the measured quantities and sizes of phosphor powder in each position. Wall loss efficiency curves for each stage could then be derived.

NUMERICAL SIMULATION OF IMPACTOR PERFORMANCE

Ludwig (1968) describes the results of computer simulation of the six-stage Andersen impactor using the efficiency curves of other workers, and taking no account of wall losses. From the calibration and wall loss investigations described above, a similar, more complete, approach was adopted for the Andersen MkI, MkII and MkII with preimpactor, with a view to improving the accuracy of airborne dust size distribution measurement. The desired end product of the exercise was a scheme for deriving the true airborne size distribution from the masses of dust collected on the impactor plates. Experimental stage calibration curves (Figs 5 and 6), and similar curves for wall deposition, were mathematically defined. (Details are given in Vaughan, 1986a, b.) An entry efficiency curve (discussed below) was assumed. A computer model was then set up of a dust cloud with log-normal size distribution being sampled by the impactor. Each 'dust cloud' was challenged successively by the entry efficiency curve, and the impaction and wall loss curves for the different stages; the mass of dust collected in each part of the impactor was then calculated. Data inversion methods conventionally applied to impactor samples could be used to reconstruct the original size distribution, and the error in size distribution measurement found.

One limitation of the computer model developed was the fact that detailed information about the entry efficiency of the Andersen impactor inlet was not available. McFarland *et al.* (1977) found virtually zero entry efficiency for $15\ \mu\text{m}$ particles when sampling with the impactor upright, at a wind speed of $15\ \text{ft s}^{-1}$ ($4.6\ \text{m s}^{-1}$), and higher efficiency at lower wind speeds. While such velocities may be typical of the outdoor environment (to which the work of McFarland *et al.* was directed) it is probably excessive for indoor working environments where a somewhat higher cut-off diameter can be expected. In the absence of any firm data, and for simplicity, the entry efficiency was assumed to be one for particles up to $20\ \mu\text{m}$, and to fall sharply to zero at this point. Experimental determination of the true entry efficiency curve would enable a more accurate computer model to be developed.

The simulation programs for each version of the impactor (MkI, MkII, and MkII with preimpactor) calculated the proportion of the incoming material which would be collected on the walls of each stage and on each plate of the impactor. In order to be directly analogous to a real sample, the proportions of material collected on the impactor plates were recalculated so as to disregard the material lost to the impactor walls. Once recalculated, the data were treated in exactly the same way as real impactor data, by plotting the cumulative % undersize against the impactor stage cut-off diameter (measured d_{50} , from Table 3) on log-probability axes. The estimated median and σ_g were then compared with those of the 'sampled' distribution which gave rise to the data. These procedures were carried out for a wide range of 'sampled' log-normal distributions, for each version of the impactor tested. Comparison of the estimated and sampled distribution parameters enabled Figs 15–23 to be drawn.

If it is accepted that the truncation of sampled distributions at $20\ \mu\text{m}$ approximates to the actual field performance of the impactor, then these figures can be used, within limits, to estimate wall losses, and to derive the true aerodynamic diameter distribution giving rise to an impactor sample. Figure 24 shows the scheme which should be used. The accuracy of the distribution parameters so derived is limited by the precision with which the figures can be read, and the assumed entry efficiency. It should also be borne in mind that the computer model assumes no bounce on impactation, and can only realistically be applied to low loadings and greased plates. Even then the model should be considered to give the minimum possible value for wall loss.

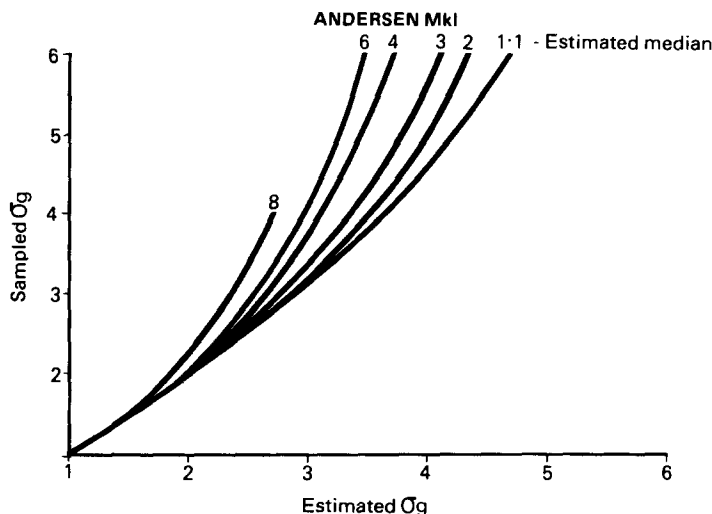


Fig. 15. For derivation of sampled σ_g from MkI impactor estimated parameters.

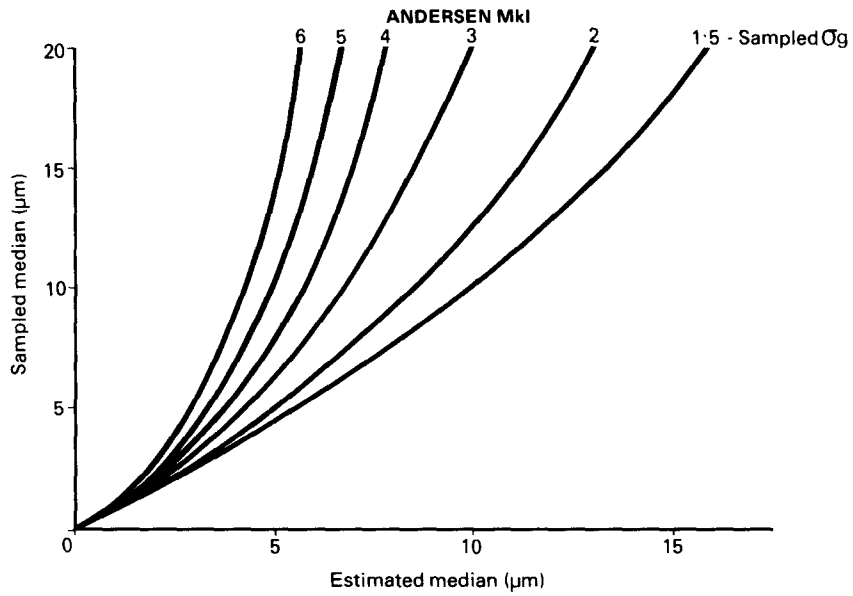


Fig. 16. Derivation of sampled median for MkI impactor.

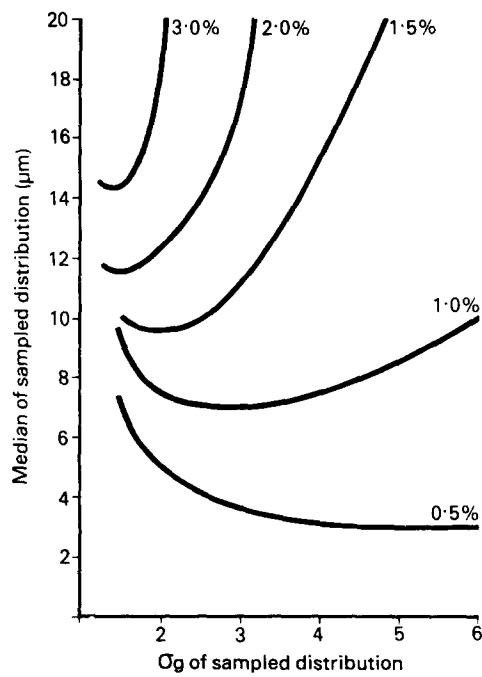


Fig. 17. Total % wall loss for MkI Andersen as a function of size distribution.

Worked example:

(1) Estimated distribution parameters for the MkII impactor sample were:

Estimated median = $5 \mu\text{m}$

Estimated $\sigma_g = 3.5$.

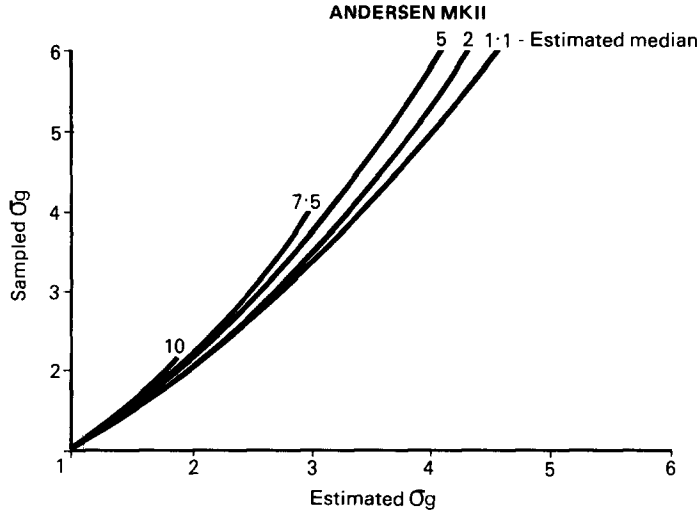


Fig. 18. Derivation of sampled σ_g from MkII impactor estimated parameters.

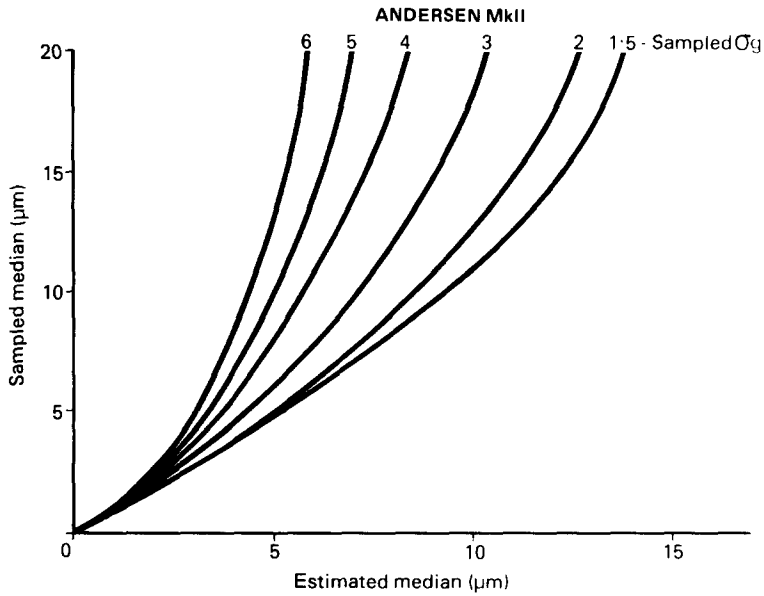


Fig. 19. Derivation of sampled median for MkII impactor.

(2) By reference to Fig. 18, this corresponds to a sampled σ_g of 4.7.

$$\text{Estimated median} = 5 \mu\text{m}$$

$$\text{Sampled } \sigma_g = 4.7.$$

(3) By reference to Fig. 19 this corresponds to an approximate sampled log-normal distribution of:

$$\text{Median} = 9 \mu\text{m}$$

$$\sigma_g = 4.7.$$

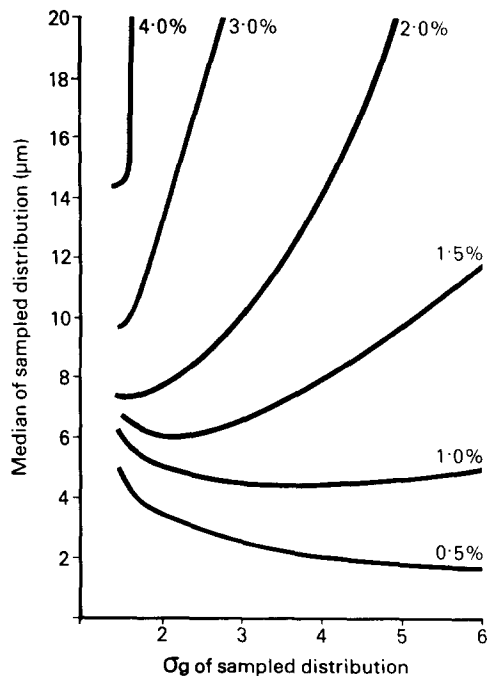


Fig. 20. Total % wall loss for MkII Andersen as a function of size distribution.

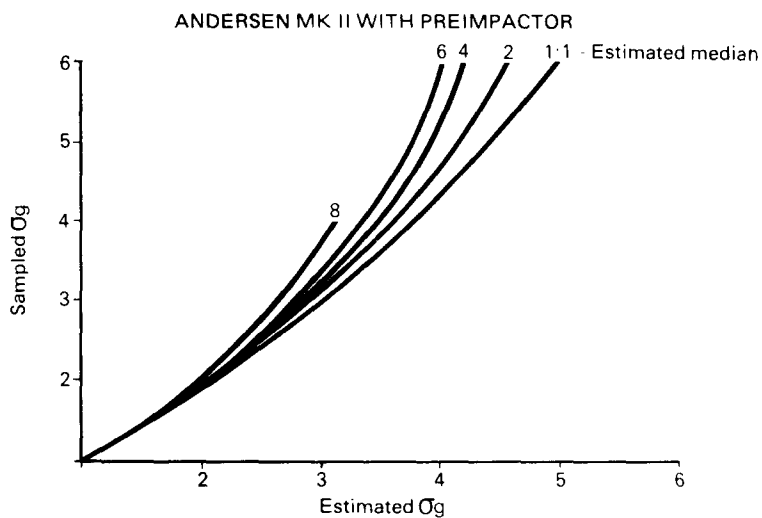


Fig. 21. Derivation of sampled σ_g from MkII + preimpactor estimated parameters.

(4) Figure 20 suggests that, for this size distribution, at least 1.5% of the incoming aerosol will be lost to the impactor walls.

CONCLUSION

Due to physical and mechanical limitations, inertial impactors can never achieve the ideal form of separation efficiency curve (i.e. a vertical step from zero efficiency for particles with lower inertia than the critical value of $\psi^{1/2}$, to 100% efficiency for particles with higher inertia). Practical sampling devices are also prone to the occurrence of wall losses. Despite

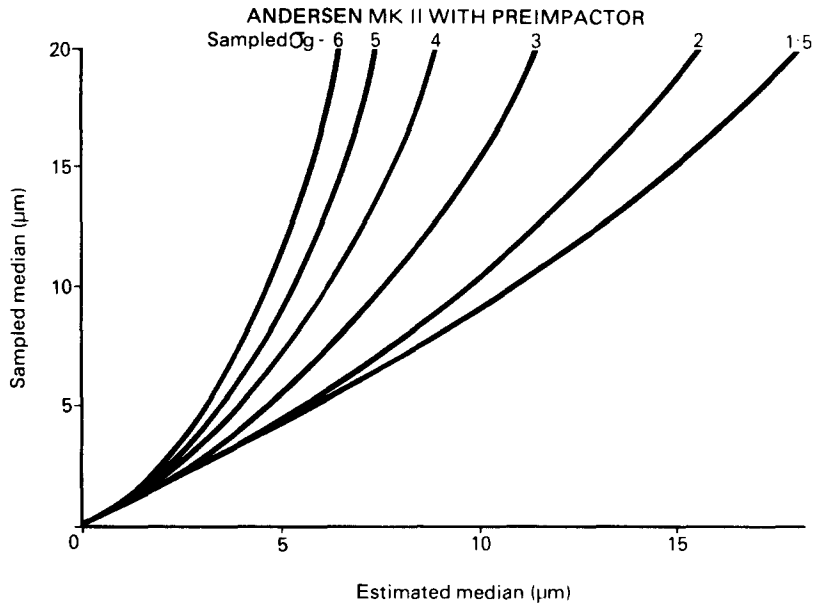


Fig. 22. Derivation of sampled median for MkII + preimpactor.

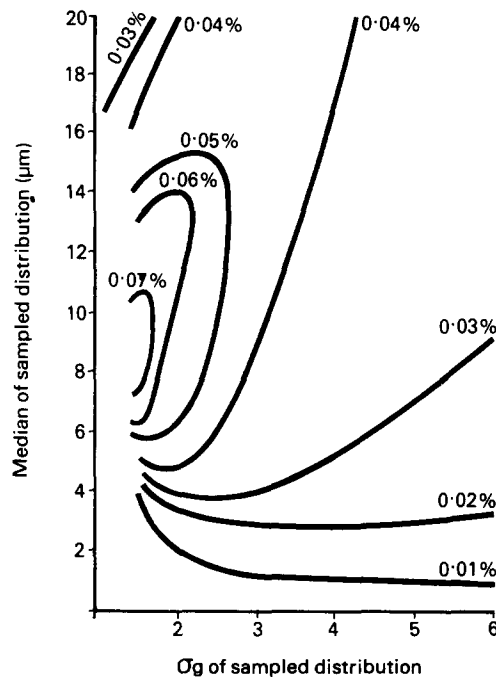


Fig. 23. Total % wall loss for MkII + preimpactor as a function of size distribution.

considerable effort by many workers, constant entry efficiency over a wide range of particle sizes and air speeds has not been achieved, and accurate entry efficiency prediction is not yet possible. These factors should be borne in mind when considering the accuracy of size distributions measured with cascade impactors.

The information given by this study should improve estimates of size distribution made with the Andersen impactors. Greater improvement could be made if their true entry efficiency under conditions of use was accurately known.

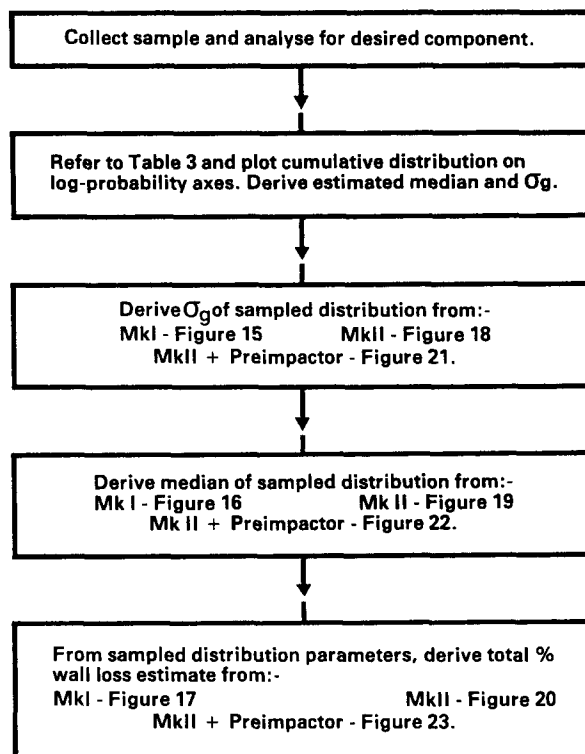


Fig. 24. Scheme of use for impactor simulation results.

REFERENCES

- Andersen, A. A. (1958) A new sampler for the collection, sizing and enumeration of viable particles. *J. Bact.* **76**, 471-484.
- Andersen, A. A. (1966) A sampler for respiratory health hazard assessment. *Am. ind. Hyg. Ass. J.* March, April, 160-165.
- Andersen 2000 Inc. (1977) Operating manual for Andersen 2000 Inc. 1ACFM ambient particle sizing samplers. Andersen 2000 Inc., Atlanta, Georgia.
- Berglund, R. N. and Liu, B. Y. H. (1973) Generation of monodisperse aerosol standards. *Envir. Sci. Technol.* **7**, 147-153.
- Boulaud, D., Diouri, M. and Madelaine, G. (1981) Parameters influencing the collection efficiency of solid aerosols in cascade impactors. *Aerosols in Science, Medicine and Technology* (Edited by Stober, W. and Hochrainer, D.), pp. 125-130. Proceedings of the 9th GAeF conference, Duisburg.
- Esmen, N. A. and Lee, T. C. (1980) Distortion of cascade impactor measured size distribution due to bounce and blow off. *Am. ind. Hyg. Ass. J.* **41**, 410-419.
- Flesch, J. P., Norris, C. H. and Nugent, A. E. (1967) Calibrating particulate air samplers with monodisperse aerosols: application to the Andersen cascade impactor. *Am. ind. Hyg. Ass. J.* November, December, 507-516.
- LeGuen, J. M. M. and Galvin, S. (1981) Clearing and mounting techniques for the evaluation of asbestos fibres by the membrane filter method. *Ann. occup. Hyg.* **24**, 273-280.
- Ludwig, F. L. (1968) Behaviour of a numerical analog of a cascade impactor. *Envir. Sci. Technol.* **2**, 547-550.
- Marple, V. A. and Liu, B. Y. H. (1974) Characteristics of laminar jet impactors. *Envir. Sci. Technol.* **8**, 648-654.
- Marple, V. A. and Willeke, K. (1976) Impactor design. *Atmos. Envir.* **10**, 891-896.
- May, K. R. (1945) The cascade impactor. An instrument for sampling coarse aerosols. *J. scient. Instrum.* **22**, 187-195.
- May, K. R. (1964) Calibration of a modified Andersen bacterial aerosol sampler. *Appl. Microbiol.* **12**, 37-43.
- May, K. R. (1975) Aerosol impaction jets. *J. Aerosol Sci.* **6**, 403-411.
- May, K. R. and Druett, H. A. (1968) A microthread technique for studying the viability of microbes in a simulated airborne state. *J. gen. Microbiol.* **51**, 353-366.
- McFarland, A. R. (1977) Fractional efficiency of selected Andersen stages. Andersen 2000 Inc., Atlanta, Georgia.
- McFarland, A. R., Wedding, J. B. and Cermak, J. E. (1977) Wind tunnel evaluation of a modified Andersen impactor and an all weather sampler inlet. *Atmos. Envir.* **11**, 535-539.
- Mitchell, J. P., Costa, P. A. and Waters, S. (1988) An assessment of the Andersen Mark-II cascade impactor. *J. Aerosol Sci.* **19**, 213-221.
- Ranz, W. E. and Wong, J. B. (1952) Impaction of dust and smoke particles on surface and body collectors. *Ind. Engng Chem.* **44**, 1371-1381.
- Rao, A. K. and Whitby, K. T. (1978a) Non-ideal collection characteristics of inertial impactors—I. Single stage impactors and solid particles. *J. Aerosol Sci.* **9**, 77-86.

- Rao, A. K. and Whitby, K. T. (1978b) Non-ideal collection characteristics of inertial impactors—II. Cascade impactors. *J. Aerosol Sci.* **9**, 87–100.
- Riediger, G. (1974) Über den Einsatz des Andersen-Kaskadenimpaktors in der gewerbehygienischen Pruftechnik, speziell zur Bestimmung des Fraktionsabscheidegrades. *Staub.* **34**, 287–291.
- Smith, M. L. (1984) (personal communication).
- Tanaka, S., Kobayashi, E. and Hashimoto, Y. (1983) Aerosol collection characteristics of the Andersen sampler for different collection surfaces. *Japan Soc. Air Pollut. J.* **18**, 256–262.
- Vaughan, N. P. (1986a) Methods for the assessment of dust hazards in metal processing industries. Ph.D. thesis, University of Leeds.
- Vaughan, N. P. (1986b) The Andersen impactor. HSE internal report*, IR/L/DS/86/7.

* HSE internal reports are available from the author on request.